

**Sensitivity of snow  
regime in  
shrub-covered valley**

C. B. Ménard et al.

This discussion paper is/has been under review for the journal Hydrology and Earth System Sciences (HESS). Please refer to the corresponding final paper in HESS if available.

# Modelled sensitivity of the snow regime to topography, shrub fraction and shrub height

C. B. Ménard<sup>1</sup>, R. Essery<sup>2</sup>, and J. Pomeroy<sup>3</sup>

<sup>1</sup>Arctic Research Centre, Finnish Meteorological Institute, Helsinki, Finland

<sup>2</sup>School of Geosciences, University of Edinburgh, Edinburgh, UK

<sup>3</sup>Centre for Hydrology, University of Saskatchewan, Saskatoon, Canada

Received: 5 December 2013 – Accepted: 13 December 2013 – Published: 7 January 2014

Correspondence to: C. B. Ménard (cecile.bauduin-menard@fmi.fi)

Published by Copernicus Publications on behalf of the European Geosciences Union.

Title Page

Abstract

Introduction

Conclusions

References

Tables

Figures

⏪

⏩

◀

▶

Back

Close

Full Screen / Esc

Printer-friendly Version

Interactive Discussion



## Abstract

Recent studies show that shrubs are colonizing higher latitudes and altitudes in the Arctic. Shrubs affect the wind transport, accumulation and melt of snow, but there have been few sensitivity studies of how shrub expansion might affect snowmelt rates and timing. Here, a blowing snow transport and sublimation model is used to simulate pre-melt snow distributions and a 3-source energy balance model, which calculates vertical and horizontal energy fluxes between the atmosphere, snow, snow-free ground and vegetation, is used to simulate melt. Vegetation is parametrized as shrub cover and the parametrization includes shrub bending and burial in winter and emergence in spring. The models are used to investigate the sensitivity of the snow regime in an upland tundra valley to varying shrub cover and topography. Results show that topography dominates the spatial variability of snow accumulation, which in turn dominates the pre and early melt energy budget. With topography removed from the simulations, modelled snow cover is uniform when there is no vegetation but increasing vegetation introduces spatial variability in snow accumulation which is then decreased as further increases in shrub cover suppress wind-induced redistribution of snow. The domain-averaged simulations of premelt snow accumulation also increases with increasing shrub cover because suppression of blowing snow by shrubs decreases sublimation. In simulations with topography, the increase in snow accumulation and its spatial variability with increasing vegetation is less marked because snow is also held in topography-driven drifts. With topography, the existence of wind-scoured snow-free patches at the onset of snowmelt causes exposed ground to contribute to the energy balance such that sensible, advective and radiative heat fluxes are higher than in the flat domain during this period. However, as snowmelt evolves, differences in the energy budget between runs with and without topography dramatically diminish. These results suggest that, to avoid overestimating the effect of shrub expansion on the energy budget of the Arctic, future large scale investigations should consider wind redistribution of snow, shrub bending and emergence, and sub-grid topography as they affect the variability of snowcover.

**HESSD**

11, 223–263, 2014

### Sensitivity of snow regime in shrub-covered valley

C. B. Ménard et al.

[Title Page](#)

[Abstract](#)

[Introduction](#)

[Conclusions](#)

[References](#)

[Tables](#)

[Figures](#)

[⏪](#)

[⏩](#)

[◀](#)

[▶](#)

[Back](#)

[Close](#)

[Full Screen / Esc](#)

[Printer-friendly Version](#)

[Interactive Discussion](#)



## 1 Introduction

The effects of shrub expansion or retreat on tundra surface energy balance have garnered much attention over the past decade. Increasing evidence from field observations, remote sensing and models suggests that warming in the Arctic has led to a “greening” that is partly due to the densification and expansion of shrub patches (Sturm et al., 2005a; Jia et al., 2006; Reynolds et al., 2006; Tape et al., 2006; Lorant et al., 2011; Tremblay et al., 2012). Chapin III et al. (2005) estimated that reductions in the duration of snow cover for arctic Alaska has increased local atmospheric heating by  $3 \text{ W m}^{-2}$  per decade, and continuation of current trends in shrub expansion could amplify this heating by two to seven times.

In addition to climate-induced changes, grazing can also control shrub coverage and height. In Northern Finland, intensive year-round reindeer grazing prevents shrub growth such that albedo during the snow season is higher than in neighbouring Norway, where more moderate seasonal grazing management practices do not limit shrub height (Kitti et al., 2009; Cohen et al., 2013). For this reason, the contribution of grazing as one of many local solutions to control shrub expansion is increasingly being advanced (Pajunen, 2009; Tape et al., 2010).

Differences and changes in shrub cover also affect the snow mass balance of tundra because the height, density and location of shrubs affect snow distributions. Shrubs increase the snow-holding capacity of the tundra by reducing near-surface wind speeds within and downwind of shrub patches (Essery et al., 1999; Sturm et al., 2001), trapping wind-blown snow around isolated patches or at the edges of large patches (Essery and Pomeroy, 2004b). Pomeroy et al. (2004) found that the standard deviation of snow water equivalent (SWE) in a sub-arctic basin increased with decreasing shrub height, decreasing cover and increasing exposure to wind. Liston et al. (2002) predicted that replacement of low-growing vegetation over a  $4 \text{ km}^2$  domain in arctic Alaska by shrubs with a 50 cm snow holding capacity would decrease domain-averaged sublimation by 68 % and increase snow depth by 14 %. Essery and Pomeroy (2004b) argued that

HESSD

11, 223–263, 2014

### Sensitivity of snow regime in shrub-covered valley

C. B. Ménard et al.

Title Page

Abstract

Introduction

Conclusions

References

Tables

Figures

◀

▶

◀

▶

Back

Close

Full Screen / Esc

Printer-friendly Version

Interactive Discussion





## Sensitivity of snow regime in shrub-covered valley

C. B. Ménard et al.

[Title Page](#)

[Abstract](#)

[Introduction](#)

[Conclusions](#)

[References](#)

[Tables](#)

[Figures](#)

[⏪](#)

[⏩](#)

[◀](#)

[▶](#)

[Back](#)

[Close](#)

[Full Screen / Esc](#)

[Printer-friendly Version](#)

[Interactive Discussion](#)



the snowpack from shrub canopies or bare ground patches even though discontinuous snow cover is known to substantially enhance snowmelt (e.g. Liston, 1995; Neumann and Marsh, 1998; Granger et al., 2002, 2006; Pomeroy et al., 2003). The solution proposed in many LSMs (e.g. see Sellers et al., 1986, for SiB, Verseghy, 1991, for CLASS) is to calculate separate energy balances for vegetation and bare ground or snow surfaces within a gridbox (so called “2-source” models). However, this does not solve the problem for landscapes with exposed vegetation and patchy snow cover. Models that calculate a single energy balance for composite snow-covered and snow-free ground are known to fail to simulate late-lying snow patches (Marsh and Pomeroy, 1996; Bewley et al., 2010). This causes two issues in model performance: excessive melt rates and modelled sensible heat fluxes that are in the opposite direction to observations for patchy snow cover. In addition, these models do not consider horizontal advection of snow mass between gridboxes by wind.

A number of modelling studies (e.g. Kaplan and New, 2006; Lawrence and Swenson, 2011; Bonfils et al., 2012) have investigated the effects of shrub expansion on snow availability, distribution and/or energy fluxes, but none have considered the effects of topography at basin or smaller scales with a high resolution model. This study aims to address this gap by setting two objectives. The first is to introduce and evaluate a new model (designated “3SOM” for **3-source model**) that addresses issues described above for energy fluxes over sparse shrub tundra canopies and heterogeneous snow cover. The model is adapted from the 2-source (shrubs and snow) model of Bewley et al. (2010), which was itself adapted for cold environments from Blyth et al. (1999), to solve three energy balances for bare ground, snow and shrubs simultaneously within each gridbox. The second objective is to investigate the sensitivity of snow accumulation and ablation to shrubs and topography. This is achieved by initializing 3SOM with outputs from an existing distributed blowing snow model DBSM (Essery and Pomeroy, 2004b). The combined models are used to estimate changes in net radiation, turbulent heat transfer and spatial distributions of SWE associated with variations in shrub cover with or without the influence of topography.

## 2 Sites and data

Model evaluation and sensitivity analyses were performed using data from a 1 km × 1 km area around a sub-arctic tundra valley, the Granger Basin (GB) in the Yukon Territory, Canada. GB lies within the larger Wolf Creek Research Basin (WCRB), a 179 km<sup>2</sup> drainage basin 15 km south of Whitehorse that has been the subject of more than 100 peer-reviewed papers and technical reports to date on cold regions hydrology (personal communication, R. Janowicz, Yukon Environment, December 2012). A digital elevation model, canopy height map and fractional vegetation cover map of GB (Fig. 1) were derived from LiDAR data obtained during an airborne campaign in August 2007. Details of the campaign and of the LiDAR data processing are available in Chasmer et al. (2008) and Hopkinson and Chasmer (2009).

The valley site is situated in the sub-alpine ecozone of WCRB and is characterized by a southwest-facing slope (13°), a northeast-facing slope (17°) and a valley bottom with a stream flowing in a southeasterly direction. Tall (1.80 m on average) willows cover the riparian zones of the valley bottom; some of these become buried under snow in the winter and spring up during melt (Pomeroy et al., 2006; Ménard et al., 2012). Birch shrubs (0.3 to 1.5 m tall) are also widespread within the basin, generally being shorter on the exposed, well-drained plateau and taller near the wet valley bottom.

Heat fluxes and snowmelt simulated at points by 3SOM were evaluated using data from spring 2003 and 2004, and the combined DBSM and 3SOM models were driven on a high-resolution grid with data from winter and spring 2007–2008. Driving and evaluation data are used from seven automatic weather stations:

1. a tall (> 2 m) shrubs station, located amongst willows in the riparian zone at 1363 m a.s.l., has been measuring meteorological data since spring 1997.
2. A short (birches of 0.32 m on average, Bewley et al., 2010) shrubs station operated in spring 2003 and 2004 only on an exposed plateau away from the drainage course at 1424 m a.s.l., approximately 330 m from the tall shrubs station.

# HESSD

11, 223–263, 2014

## Sensitivity of snow regime in shrub-covered valley

C. B. Ménard et al.

[Title Page](#)

[Abstract](#)

[Introduction](#)

[Conclusions](#)

[References](#)

[Tables](#)

[Figures](#)

[⏪](#)

[⏩](#)

[◀](#)

[▶](#)

[Back](#)

[Close](#)

[Full Screen / Esc](#)

[Printer-friendly Version](#)

[Interactive Discussion](#)



## Sensitivity of snow regime in shrub-covered valley

C. B. Ménard et al.

Title Page

Abstract

Introduction

Conclusions

References

Tables

Figures

⏪

⏩

◀

▶

Back

Close

Full Screen / Esc

Printer-friendly Version

Interactive Discussion

3. Two stations situated on opposite slopes of the valley, one on the southwest-facing slope and the other on the northeast-facing slope. They were operated in spring 2003 and 2004 only.
4. A second short shrub plateau station which was installed in Summer 2007 near where the previous short shrub station had been located.
5. A sparse tundra alpine station at 1560 m a.s.l. and 3 km from the valley, operated between Autumn 1993 and Summer 2009. The alpine zone has dwarf vegetation and barren ground.
6. Environment Canada make regular meteorological observations at Whitehorse International airport (“WIA”) (Environment Canada – National Climate Data and Information Archive, 2012), 19 km from GB and 590 m lower in elevation.

The locations of stations 1 to 4 are shown on Fig. 1. Air temperature  $T_a$ , wind speed  $u$ , wind direction  $u_{dir}$ , relative humidity RH, incoming shortwave radiation  $SW_{in}$ , incoming longwave radiation  $LW_{in}$  and snow depth  $S_d$  were measured every half hour at the tall and short shrub stations. Data from the alpine station were used to fill gaps in wind speed and direction data required by the blowing snow model. As wind data were missing from both the second plateau and the alpine stations for 42 consecutive days from January to mid-February 2008, the missing data were infilled with data collected at WIA. Daily snowfall measurements were not made within the Wolf Creek basin during the study period, so snowfall data were obtained from the WIA meteorological station. A correction factor for differences in snowfall between GB and WIA due to the difference in elevation was applied to the snowfall rate, as detailed in Ménard et al. (2012).

Sensible and latent heat fluxes measured by eddy covariance towers at the tall and short shrubs stations in spring 2003 and 2004 are compared with point simulations in Sect. 3.3. A ground heat flux plate also provided measurements at the short shrub station in 2003. Data from the slope stations are used to evaluate the modelled distribution of incoming shortwave radiation (discussed in Sect. 4.1). Snow depths were measured

every 5 m and snow density every 25 m with an ESC-30 snow tube along three transects (Fig. 1) of approximately 400 m length. In 2008, the transects were monitored every three to four days during the melt season until all the snow, except in drifts on the northeast-facing slope, had melted. The transect measurements are used to evaluate simulations of snow depth before and during melt in Sect. 4.2.

### 3 Three-source model description and evaluation

This section describes the surface, snow and soil schemes of 3SOM, represented schematically in Fig. 2, and presents an evaluation of point simulations against heat flux and snowmelt measurements in spring 2003 and 2004.

#### 3.1 Surface scheme

The surface scheme has separate energy balances for snow, bare ground and exposed vegetation sources coupled through a network of resistances, allowing horizontal and vertical transfer of heat between sources within a gridbox. Following the convention that radiative fluxes are positive towards the surface and turbulent and ground heat fluxes are positive away from the surface, the separate energy balance equations for vegetation, snow-free ground and snow, identified by subscripts  $v$ ,  $g$  and  $s$  respectively, are

$$R_v = H_v + LE_v \quad (1)$$

$$R_g = H_g + LE_g + G_g \quad (2)$$

$$R_s = H_s + LE_s + G_s + M_s \quad (3)$$

where  $R$  is the net radiation,  $H$  and  $LE$  are the sensible and latent heat fluxes respectively,  $M$  is the snowmelt heat flux,  $G_g$  is the heat flux from the soil to the soil surface and  $G_s$  from the snowpack to the snow surface. Averaged over a gridbox with exposed vegetation fraction  $F_v$ , snow cover fraction  $F_s$  and snow-free ground fraction  $F_g = (1 - F_s)$ ,

## Sensitivity of snow regime in shrub-covered valley

C. B. Ménard et al.

Title Page

Abstract

Introduction

Conclusions

References

Tables

Figures

⏪

⏩

◀

▶

Back

Close

Full Screen / Esc

Printer-friendly Version

Interactive Discussion



the net radiation is

$$R = F_v R_v + F_s R_s + F_g R_g \quad (4)$$

the total moisture flux, ignoring evaporation from dormant vegetation, to the atmosphere is

$$E = F_s E_s + F_g E_g \quad (5)$$

and, thus allowing advection from snow-free to snow-covered surfaces, the sensible heat flux is

$$H = F_v H_v + F_s H_s + F_g H_g \quad (6)$$

The parametrizations of fluxes in Eqs. (1) to (5) are very similar to those in the 2-source model of Bewley et al. (2010) and can be found in the Appendix.

The Yang et al. (1997) parametrization

$$F_s = \tanh\left(\frac{S_d}{\chi}\right) \quad (7)$$

is used for snow cover fraction, where  $S_d$  is snow depth (m) and  $\chi = 0.17$  m is a parameter fitted to GB snow survey data by Ménard et al. (2012). The exposed vegetation fraction, allowing for bending and burial of shrubs by snow, is taken from Liston and Hiemstra (2011) such that

$$F_v = F_{v0} \max\left[0, \left(1 - \frac{S_d}{h_c B}\right)\right] \quad (8)$$

where  $F_{v0}$  is the snow-free vegetation fraction,  $h_c$  is canopy height and  $B = 0.85$  is a bending parameter estimated by Ménard et al. (2012) for the valley site in the 2007–2008 season.

## HESSD

11, 223–263, 2014

### Sensitivity of snow regime in shrub-covered valley

C. B. Ménard et al.

Title Page

Abstract

Introduction

Conclusions

References

Tables

Figures

◀

▶

◀

▶

Back

Close

Full Screen / Esc

Printer-friendly Version

Interactive Discussion



## 3.2 Snow and soil schemes

The snow and soil thermodynamics schemes used in 3SOM to calculate  $G_s$  and  $G_g$  are taken from the Joint UK Land Environment Simulator (JULES, Best et al., 2011). The number of model layers is adjustable in JULES, but 4 soil layers extending to 1.5 m depth and up to 3 snow layers are used here. Each layer has a temperature, a liquid water content and a frozen water content. The thickness of the snow layers varies as snow compacts or fresh snow accumulates. The snow albedo parametrization used in 3SOM differs from that in JULES, instead using the simpler parametrization of Douville et al. (1995). The albedo of snow decreases over time, at a faster rate for melting than cold snow, and is refreshed to the albedo of fresh snow by the accumulation of  $10 \text{ kg m}^{-2}$  of snowfall. The three surface sources share a single soil column per gridbox. Transfers of heat and water between columns are neglected; this makes the model unsuitable for distributed hydrological modelling over complex topography but has little impact on the simulations of turbulent fluxes and snowmelt that are the focus of this paper.

## 3.3 Evaluation of the model at points

3SOM is first evaluated against observations at the tall and short shrubs stations throughout the melt periods of 2003 and 2004, using manual measurements of vegetation height and initial snow depths at the stations. Results are presented in Fig. 3. Modelled SWE and snow depth are closer to measurements in 2004 than in 2003. Melt started earlier in 2003 and the snow at the short shrubs site had disappeared by 30 April, but melt at the tall shrubs site stagnated because of a drop in air temperature between 30 April and 6 May. Although melt rates are overestimated at both stations in 2003, 3SOM is still able to reproduce late-lying snow at the tall shrubs site, albeit shallower than measured. Modelled melt rates are 73% larger at the tall than at the short shrubs site in 2003 and 64% larger in 2004 on average due to advection of heat from the shrubs to the snow.

HESSD

11, 223–263, 2014

### Sensitivity of snow regime in shrub-covered valley

C. B. Ménard et al.

Title Page

Abstract

Introduction

Conclusions

References

Tables

Figures

◀

▶

◀

▶

Back

Close

Full Screen / Esc

Printer-friendly Version

Interactive Discussion



## Sensitivity of snow regime in shrub-covered valley

C. B. Ménard et al.

Title Page

Abstract

Introduction

Conclusions

References

Tables

Figures

◀

▶

◀

▶

Back

Close

Full Screen / Esc

Printer-friendly Version

Interactive Discussion

In both years, the model is able to reproduce the direction and magnitude of energy exchanges with the atmosphere over a dynamic surface. Contributions of the individual sources to energy fluxes are shown in Fig. 4. At the short shrubs site,  $H_g$  from a small snow-free fraction is positive during daytime from the beginning of the run but  $H_v$  is negligible because little vegetation is exposed and total sensible heat fluxes (measured and modelled) are predominantly negative until the snow has melted. At the tall shrubs site,  $H$  is positive during daytime owing to large upwards heat fluxes from exposed vegetation and negative at night, with heat transferred from the atmosphere to both snow and vegetation. Downwards sensible heat fluxes at night are slightly overestimated by the model, particularly at the tall shrubs site. Latent heat fluxes from snow and bare ground are upwards during the day and small at night for both sites.

On 24 and 25 April 2003 and from 1 to 3 May 2004, modelled and measured sensible heat fluxes at the short shrubs site are in opposite directions. Bewley et al. (2010) suggested that this occurs if models are unable to simulate separate energy balances for coexisting snow patches and snow-free ground. 3SOM does have fractional snow cover and positive  $H_g$  for these dates, but the area-average  $H$  is dominated by negative  $H_s$  (Fig. 4). The magnitude and duration of anomalous fluxes are greatly reduced in 3SOM simulations compared with 2-source simulations for the same periods at the short shrubs site presented by Bewley et al. (2010).

Table 1 shows quantitative assessments of the modelled fluxes. Although some of the errors are large, turbulent fluxes modelled at points have been compared here with measurements that are influenced by heterogeneous upwind surface conditions. Ideally, a footprint model should be used to weight the modelled fluxes for comparison with measurements. However, accurate determination of the measurement footprint and flux sources would constitute an entirely separate study. Given the differences in scale between the point model and the flux measurements and the correspondence between the two, the model is judged to perform well enough at a point to use it in distributed simulations over a landscape.

## 4 Description and evaluation of distributed simulations

This section describes how meteorological data are adjusted for driving distributed simulations and presents results obtained using DBSM to simulate the evolution of accumulating snow from September 2007 to April 2008 and then using 3SOM to simulate snowmelt through April and May 2008. The sequential coupling of the models captures the dominant snow processes in each season but neglects any winter melt or spring redistribution events; a full coupling of the models is in development.

DBSM calculates changes in SWE within a gridbox over time as

$$\frac{\partial \text{SWE}}{\partial t} = S_f - q_s - \nabla \cdot \mathbf{q}_t \quad (9)$$

where  $S_f$  is the snowfall rate,  $q_s$  is the rate of sublimation from blowing snow and  $\mathbf{q}_t$  is the rate of mass transport by blowing snow. Parametrizations of the blowing snow fluxes depending on local wind speed, vegetation height, erodability of the snow surface, air temperature and relative humidity are described by Essery et al. (1999), Pomeroy and Li (2000), Essery and Pomeroy (2004b).

### 4.1 Distribution of the driving data

The models were run on an 8 m grid covering a 1 km × 1 km domain, with the elevation, vegetation fraction and vegetation height of each gridbox obtained from LiDAR data. Some of the slopes in GB are in excess of 20° but the altitude range is less than 260 m, so only the incoming shortwave radiation and the wind speed are distributed for model driving; Pomeroy et al. (2003) measured all of the meteorological forcing variables on different slopes and at different elevations in the basin and found this to be a reasonable assumption.

Measurements of total incoming shortwave radiation made with a levelled radiometer at the tall shrubs site were partitioned into diffuse and direct components following the empirical method proposed by Erbs et al. (1982) and adjusted for the slope and aspect

**HESSD**

11, 223–263, 2014

## Sensitivity of snow regime in shrub-covered valley

C. B. Ménard et al.

Title Page

Abstract

Introduction

Conclusions

References

Tables

Figures

◀

▶

◀

▶

Back

Close

Full Screen / Esc

Printer-friendly Version

Interactive Discussion



of each gridbox according to the solar elevation and azimuth for each timestep as described by Oke (1987) and Liston and Elder (2006). Comparisons between predictions and measurements made parallel to the slopes at the slope stations in 2003 are shown in Fig. 5.

Wind speeds were distributed using the Mason and Sykes (1978) model of flow over topography, which requires wind speed and direction at an exposed location as inputs. These data were taken from measurements at the plateau station when available and gaps were filled with data from the alpine or WIA stations. Average wind directions for periods of overlapping data at these stations were within the  $45^\circ$  discretization of wind directions used by DBSM. Average wind speed at WIA differed from the plateau station by only  $0.16 \text{ ms}^{-1}$  but was  $1.18 \text{ ms}^{-1}$  higher at the alpine station. Wind speeds at the alpine station were multiplied by a factor of 0.77 found by minimizing the difference between measured and DBSM modelled snow depths used as initial conditions for 3SOM.

## 4.2 Evaluation of distributed simulations

DBSM was run from 1 September 2007 to 19 April 2008 to generate SWE and snow depth grids as initial conditions for melt simulations by 3SOM, which was then run from 19 April to 28 May. Lacking distributed measurements or an adequate model of below-ground heat and water transport, the soil temperature was initialized to the measured temperature at the tall shrubs site (the soil temperature at the plateau station on 19 April only differed by  $2^\circ\text{C}$  despite different snow conditions). As a simple method of making the valley bottom wetter than the plateau, initial soil moisture content  $\theta$  was scaled according to a topographic index (Kirkby and Weyman, 1974; Beven and Kirkby, 1979) such that  $\theta = \theta_{\text{sat}} \text{TI} / \text{TI}_{\text{max}}$ , where  $\theta_{\text{sat}}$  is the volumetric soil moisture content at saturation and  $\text{TI}_{\text{max}}$  is the maximum value of topographic index found within the domain.

Modelled snow depths and standard deviation of snow depths are compared with manual measurements and discretized per melt period and three topographic fea-

## Sensitivity of snow regime in shrub-covered valley

C. B. Ménard et al.

Title Page

Abstract

Introduction

Conclusions

References

Tables

Figures

◀

▶

◀

▶

Back

Close

Full Screen / Esc

Printer-friendly Version

Interactive Discussion



tures: the northeast-facing slope (NFS), the valley and the southwest-facing slope (SFS) (Fig. 6). Although the broad features of snow distribution and disappearance are captured, there are large some errors in both space and time; errors in snow depths increase during melt but decrease at the end of melt and the model systematically underestimates the standard deviation. The simulated disappearance of snow from the southwest-facing slope later than observed is consistent with the overestimation of snow depth before the start of melt. This may occur because the model only accounts for atmospheric advection of heat within and not between gridboxes. Warming of air by upwards sensible heat fluxes over snow-free patches and warming of snow by downwards heat fluxes as the air then passes over snow patches is a process that has been well documented at GB (Granger et al., 2002, 2006; Essery et al., 2006). Figure 7 shows the southwest-facing slope on three dates during the first two weeks of the melt season; the red arrow points to a snow-free patch close to one of the transects that was small enough on 20 April to be contained within a single model gridbox but had grown much larger by 27 April.

3SOM performed well in the point simulations at the tall and short shrubs sites with initial snow depth, SWE, vegetation fraction and vegetation height specified from direct measurements. A number of factors could contribute to errors and some of the poor quantitative statistics in Table 2 in the distributed simulations. Firstly, scale between model and observations differ; measurements are points whereas model output covers 8 m × 8 m gridboxes. Secondly, the snow surveys were conducted as close as possible to the previous surveys but individual points generally differed by a few centimeters (between 5 cm to 1 m) because of the destructive nature of sampling snow density and depth; Fig. 6 shows measurements errors as measured mean snow depth at the end of melt on the northeast-facing slope is higher than during melt. Finally, given the high resolution of the model, small errors in the LiDAR mapping of topography and vegetation will have some influence on model results.

## HESSD

11, 223–263, 2014

### Sensitivity of snow regime in shrub-covered valley

C. B. Ménard et al.

Title Page

Abstract

Introduction

Conclusions

References

Tables

Figures

⏪

⏩

◀

▶

Back

Close

Full Screen / Esc

Printer-friendly Version

Interactive Discussion



## 5 Effects of shrub expansion

Despite issues discussed above, the DBSM and 3SOM models are able to capture the evolution of broad spatial snow patterns across GB and diurnal and seasonal variations in energy fluxes at two points representative of short and tall shrub cover within GB. The models are now used in a sensitivity study investigating the effects of shrub expansion on snow distribution and energy balance, with and without topography.

Shrub expansion can proceed by infilling and lateral growth of existing shrub patches, increase in the height of shrubs and colonisation of areas beyond the shrubline (Tape et al., 2006; Myers-Smith et al., 2011). Without going to the complexity of introducing an ecological model, shrub expansion by the first two mechanisms was simulated by iteratively increasing the area and height of existing shrubs in the Granger valley for perturbed simulations. In each iteration, the vegetation fraction and height in each model gridbox were increased by a random amount up to the maxima in any of the eight neighbouring boxes. This process was repeated 20 times, saving vegetation fraction and height maps after 1, 3, 5, 10 and 20 iterations; the vegetation fraction increases from 8 % in the LiDAR-derived map to 52 % after 20 iterations. DBSM and 3SOM runs were performed without vegetation, with existing vegetation, and with each of the five increased vegetation scenarios. Two runs were performed in each case: one with the existing topography and one on a flat domain. Model outputs were averaged over the central 1 km<sup>2</sup> of the domain.

Premelt conditions on 22 April are shown in Fig. 8. About one third of the vegetation is buried by snow in each case, with little impact of topography. With no vegetation and no topography, DBSM calculates sublimation of blowing snow but no net redistribution within the domain. As the vegetation fraction is increased for the flat domain, the domain-average premelt SWE increases because the reduction of near-ground wind speed by shrubs decreases blowing snow sublimation. In runs with topography, the increase in SWE with increasing  $F_v$  is much less marked because deposition of snow also occurs in areas of decreased wind speed, such as hillslopes and depressions

HESSD

11, 223–263, 2014

### Sensitivity of snow regime in shrub-covered valley

C. B. Ménard et al.

Title Page

Abstract

Introduction

Conclusions

References

Tables

Figures

⏪

⏩

◀

▶

Back

Close

Full Screen / Esc

Printer-friendly Version

Interactive Discussion



and reduces the possible deposition in the tall shrubs of the valley bottom; Quinton et al. (2004) estimated that the large drift near the top of the northeast-facing slope can store up to 65% of the snow mass in the Granger valley. For  $F_v > \approx 0.4$ , average premelt SWE is similar for runs with or without topography and is controlled by the shrubs. Spatial variability in premelt SWE can be characterized by the coefficient of variation (CV = standard deviation divided by mean). In simulations without topography, the snow cover is uniform when there is no vegetation (CV = 0 when  $F_v = 0$ ), but CV first increases as increasing shrub cover introduces some spatial variability in snow accumulation and then decreases as further increases in vegetation suppress wind-induced redistribution of snow. Variability reaches a maximum without vegetation in simulations with topography and drops to CV = 0.29 at  $F_v = 0.52$ . In comparison, Pomeroy et al. (2004) found CV = 0.27 from snow surveys for well-vegetated sites in WCRB.

The average pre-melt SWE is important because it determines how much energy is required to melt all of the snow, but spatial variability in premelt SWE is also important because it determines how much snow-free ground is exposed after a certain amount of snow has melted (Pomeroy et al., 1998; Essery and Pomeroy, 2004a) and hence influences the surface energy partitioning. Time series of snow cover fraction and snow cover depletion curves ( $F_s$  plotted against SWE) are shown for selected simulations in Fig. 9. With no topography and no vegetation, the premelt SWE and spatial distribution of melt energy are uniform and there is a rapid transition during melt from near-complete snow cover before 7 May to nearly no snow cover after 14 May; the snow cover depletion curve is simply determined by Eq. (7). The simulation with topography but without vegetation has the highest premelt CV, giving a flattened snow cover depletion curve and a much more gradual decrease in snow cover; some ground is exposed early as shallow snow melts but some snow cover persists late into May in deep drifts. Increasing vegetation fraction increases premelt SWE and decreases CV, delaying the onset of snow cover depletion but increasing its rate once it has begun because of advected energy from exposed shrubs.

## HESSD

11, 223–263, 2014

### Sensitivity of snow regime in shrub-covered valley

C. B. Ménard et al.

[Title Page](#)

[Abstract](#)

[Introduction](#)

[Conclusions](#)

[References](#)

[Tables](#)

[Figures](#)

[⏪](#)

[⏩](#)

[◀](#)

[▶](#)

[Back](#)

[Close](#)

[Full Screen / Esc](#)

[Printer-friendly Version](#)

[Interactive Discussion](#)



## Sensitivity of snow regime in shrub-covered valley

C. B. Ménard et al.

[Title Page](#)

[Abstract](#)

[Introduction](#)

[Conclusions](#)

[References](#)

[Tables](#)

[Figures](#)

[⏪](#)

[⏩](#)

[◀](#)

[▶](#)

[Back](#)

[Close](#)

[Full Screen / Esc](#)

[Printer-friendly Version](#)

[Interactive Discussion](#)



Figure 10 shows net radiation, sensible heat and latent heat fluxes averaged over early melt (22 April–4 May), main melt (5–16 May) and late melt (17–28 May) periods in simulations with and without topography. During the early melt period, the snow cover in simulations without topography is nearly complete ( $F_s \approx 1$  in Fig. 8) and the sensible heat is dominated by downward fluxes from the atmosphere to the snow; this is offset by increasing upwards sensible heat fluxes from the vegetation with increasing vegetation fractions. In simulations with topography and low vegetation fractions, the snow cover is already incomplete ( $F_s < 1$ ) on 22 April, giving upwards sensible heat fluxes from snow-free ground that offset the downwards fluxes to snow and reduce the sensitivity of overall sensible heat to vegetation fraction. In simulations with and without topography, the increase in net radiation with increasing shrub cover is largely balanced by less-negative sensible heat fluxes. Latent heat fluxes increase slightly with increasing shrub cover due to advection of heat from exposed vegetation to snow within the same gridbox.

The relationship between simulations with and without topography changes during the main melt period; almost no differences in  $R_n$  remain and sensible heat fluxes in simulations without topography are now almost independent of vegetation fractions less than 0.4. All simulations estimate less than 50 % snow cover by the end of this period, and those without topography have smaller snow cover fractions than those with topography and the same vegetation fractions because of lower initial SWE and more rapid snow depletion. Advection between gridboxes, if introduced in the model, would likely have the greatest influence during this period when there are significant fluxes from vegetation and snow-free ground but significant snow cover still remains.

There are only small differences in fluxes averaged over the late melt period between simulations with and without topography because the surface is dominated by snow-free ground and vegetation. Sensible heat fluxes increase due to increasing surface roughness with increasing vegetation fractions but latent heat fluxes decrease slightly due to a decrease in the fraction of late-lying snow patches. Because the model lacks

a hydrology module, partitioning of available energy between latent and sensible heat fluxes for snow-free ground is uncertain.

## 6 Discussion and conclusions

Corroborating previous findings (e.g. Chapin III et al., 2005; Liston and Hiemstra, 2011; Bonfils et al., 2012) this study suggests that expansion and densification of tundra shrub patches in a warming climate will have a positive feedback on warming through decreases in surface albedo and increases in sensible heat fluxes to the atmosphere. This change in surface energetics with warming is predicted despite the inclusion of a shrub bending parameterization which reduces the exposed vegetation fraction and increases the albedo at the beginning of the snowmelt season. However, topography was found to moderate the magnitude of the effects of shrub expansion on pre-melt energy budgets and snow accumulations; for the domain studied here, wind-blown snow from the exposed plateau can be trapped in a topographic drift on the northeast-facing slope before it reaches shrubs in the sheltered valley bottom. Therefore the positive feedback identified in studies of arctic plains is expected to be dampened in arctic mountains such as in the Yukon Territory and adjacent Mackenzie Mountains in NW Canada.

These findings have a number of implications for studies investigating shrub expansion over larger scales. Most climate models do not account for the effects of sub-grid topography on snow distribution because of computational constraints. Many LSMs simply parametrize sub-grid snow cover fraction as a function of SWE or snow depth, and no climate model explicitly represents sub-grid redistribution of snow by wind. The effects of vegetation on surface albedo and roughness are considered, but, with the exception of the study conducted by Lawrence and Swenson (2011) using CLM4, its effects on redistribution of snow are neglected. The exceptionally high resolution of the grid used here allowed influences of topography and vegetation on snow accumulation

# HESSD

11, 223–263, 2014

## Sensitivity of snow regime in shrub-covered valley

C. B. Ménard et al.

[Title Page](#)

[Abstract](#)

[Introduction](#)

[Conclusions](#)

[References](#)

[Tables](#)

[Figures](#)

[◀](#)

[▶](#)

[◀](#)

[▶](#)

[Back](#)

[Close](#)

[Full Screen / Esc](#)

[Printer-friendly Version](#)

[Interactive Discussion](#)





tinuous shrub and snow cover (Liston, 2004; Essery et al., 2005; Bewley et al., 2010) by calculating separate energy balances for snow, bare ground and vegetation. The study was conducted at a single location, and further studies are required to confirm the relevance of these findings in other sub-arctic and arctic environments. In addition, further work should focus on year-round changes to the energy budget associated with shrub cover and topography. Further model developments, such as adding a hydrology module, accounting for heat advection between gridboxes and fully coupling 3SOM and DBSM, will be required to further improve our understanding of the surface and soil processes associated with shrub expansion.

## Appendix

Neglecting multiple reflections between the vegetation and the ground or snow, net solar radiation absorbed at the surface is

$$SW_s = \tau(1 - \alpha_s)SW_{in} \quad (1)$$

for the snow tile,

$$SW_v = (1 - \alpha_v)SW_{in} \quad (2)$$

for the vegetation tile and

$$SW_g = \tau(1 - \alpha_g)SW_{in} \quad (3)$$

for the ground tile, where  $SW_{in}$  is the incoming shortwave radiation,  $\tau$  is the canopy transmissivity and  $\alpha$  is the albedo. Unlike Bewley et al. (2010), who used a time-averaged  $\tau$  calculated from hemispherical photographs for their point model evaluation,

## Sensitivity of snow regime in shrub-covered valley

C. B. Ménard et al.

Title Page

Abstract

Introduction

Conclusions

References

Tables

Figures

◀

▶

◀

▶

Back

Close

Full Screen / Esc

Printer-friendly Version

Interactive Discussion



$\tau$  is calculated here as a function of exposed vegetation fraction

$$\tau = \exp(-0.92F_v) \quad (4)$$

following Bewley et al. (2007). Longwave radiation is emitted both upwards and downwards from the vegetation canopy, so the net longwave radiation for vegetation temperature  $T_v$  is

$$LW_v = LW_{in} - 2\sigma T_v^4 + \sigma T_s^4 + \sigma T_g^4. \quad (5)$$

Including absorption of longwave radiation from the vegetation and the atmosphere, the net longwave radiation for the snow and vegetation surfaces is

$$LW_s = (1 - F_v)LW_{in} + F_v\sigma T_v^4 - \sigma T_s^4 \quad (6)$$

and

$$LW_g = (1 - F_v)LW_{in} + F_v\sigma T_v^4 - \sigma T_g^4 \quad (7)$$

where  $T_s$  and  $T_g$  are the snow and ground surface temperatures.

The sensible heat fluxes at the snow, bare ground and vegetation surfaces are respectively

$$H_s = \frac{\rho C_p}{r_{as}}(T_s - T_c), \quad (8)$$

$$H_g = \frac{\rho C_p}{r_{ag}}(T_g - T_c) \quad (9)$$

and

$$H_v = \frac{\rho C_p}{r_{av}}(T_v - T_c) \quad (10)$$



where  $\lambda_{\text{soil}}$  and  $\lambda_{\text{snow}}$  are the thermal conductivities of surface soil and snow layers of temperature  $T_{g1}$  and  $T_{s1}$  and thickness  $\Delta z_{g1}$  and  $\Delta z_{s1}$ . Details of the snow and soil thermodynamics can be found in Best et al. (2011).

An implicit solution is used to find increments in surface temperatures over each model timestep. The flux parametrizations in this appendix are linearized in temperature and humidity increments (using the Clausius-Clapeyron equation to expand  $Q_{\text{sat}}$ ) and substituted into the balance Eqs. (1)–(3), (5) and (6). This gives five equations for five unknowns (increments in vegetation, snow and ground surface temperatures, and temperature and humidity increments in the canopy air space) that are solved using LU decomposition (Press et al., 1996). A first solution is found assuming no snowmelt; if this gives a snow surface temperature greater than  $0^\circ\text{C}$ , the solution is repeated assuming  $T_s = 0^\circ\text{C}$  and the residual of the energy balance is used to melt snow at rate  $M_s$ .

*Acknowledgements.* This work was supported by the CFCAS research network Improved Processes and Parameterisation for Prediction in Cold Regions (IP3), the Natural Environment Research Council (NERC) grants NER/S/D/2006/14319 and NE/H000437/1, and the Nordic Centre of Excellence TUNDRA funded by the Norden Top Level Research Initiative. The authors would like to thank: Ric Janowicz, Yukon Environment, Raoul Granger and Newell Hedstrom of Environment Canada for their logistical support and the ongoing maintenance of the Granger basin; Sean Carey for providing many indispensable datasets; Jessica Boucher, Qian Chen, Shawn MacDonald and Mike Treberg for their invaluable assistance on the field.

## References

- Baker, D., Skaggs, R., and Ruschy, D.: Snow depth required to mask underlying surface, *J. Appl. Meteorol.*, 30, 387–392, 1991. 226
- Best, M. J., Pryor, M., Clark, D. B., Rooney, G. G., Essery, R. L. H., Ménard, C. B., Edwards, J. M., Hendry, M. A., Porson, A., Gedney, N., Mercado, L. M., Sitch, S., Blyth, E., Boucher, O., Cox, P. M., Grimmond, C. S. B., and Harding, R. J.: The Joint UK Land Envi-

## HESSD

11, 223–263, 2014

### Sensitivity of snow regime in shrub-covered valley

C. B. Ménard et al.

Title Page

Abstract

Introduction

Conclusions

References

Tables

Figures

⏪

⏩

◀

▶

Back

Close

Full Screen / Esc

Printer-friendly Version

Interactive Discussion



## Sensitivity of snow regime in shrub-covered valley

C. B. Ménard et al.

Title Page

Abstract

Introduction

Conclusions

References

Tables

Figures

◀

▶

◀

▶

Back

Close

Full Screen / Esc

Printer-friendly Version

Interactive Discussion



- ronment Simulator (JULES), model description – Part 1: Energy and water fluxes, *Geosci. Model Dev.*, 4, 677–699, doi:10.5194/gmd-4-677-2011, 2011. 232, 244, 245
- Beven, K. and Kirkby, M.: A physically based, variable contributing area model of basin hydrology, *Hydrological Sciences Bulletin*, 24, 43–69, 1979. 235
- 5 Bewley, D., Pomeroy, J., and Essery, R.: Solar radiation transfer through a subarctic shrub canopy, *Arct. Antarct. Alp. Res.*, 39, 365–374, 2007. 226, 243
- Bewley, D., Essery, R., Pomeroy, J., and Ménard, C.: Measurements and modelling of snowmelt and turbulent heat fluxes over shrub tundra, *Hydrol. Earth Syst. Sci.*, 14, 1331–1340, doi:10.5194/hess-14-1331-2010, 2010. 226, 227, 228, 231, 233, 241, 242, 244
- 10 Blyth, E. M., Harding, R. J., and Essery, R.: A coupled dual source GCM SVAT, *Hydrol. Earth Syst. Sci.*, 3, 71–84, doi:10.5194/hess-3-71-1999, 1999. 227
- Bonfils, C. J. W., Phillips, T. J., Lawrence, D. M., Cameron-Smith, P., Riley, W. J., and Subin, Z. M.: On the influence of shrub height and expansion on northern high latitude climate, *Environ. Res. Lett.*, 7, 015503, doi:10.1088/1748-9326/7/1/015503, 2012. 227, 240
- 15 Chapin, F., McGuire, A., Randerson, J., Pielke, R., Baldocchi, D., Hobbie, S., Roulet, N., Eugster, W., Kasischke, E., Rastetter, E., Zimov, S., and Running, S.: Arctic and boreal ecosystems of western North America as components of the climate system, *Glob. Change Biol.*, 6, 211–223, 2000. 241
- Chapin III, F., Sturm, M., Serreze, M., Chapin III, F. S., Sturm, M., Serreze, M. C., McFadden, J. P., Key, J. R., Lloyd, A. H., McGuire, A. D., Rupp, T. S., Lynch, A. H., Schimel, J. P., Beringer, J., Chapman, W. L., Epstein, H. E., Euskirchen, E. S., Hinzman, L. D., Jia, G., Ping, C.-L., Tape, K. D., Thompson, C. D. C., Walker, D. A., and Welker, J. M.: Role of land-surface changes in Arctic summer warming, *Science*, 310, 657–660, 2005. 225, 240
- 20 Chasmer, L., Hopkinson, C., Treitz, P., McCaughey, H., Barr, A., and Black, A.: A lidar-based hierarchical approach for assessing MODIS fPAR, *Remote Sens. Environ.*, 112, 4344–4357, 2008. 228
- 25 Clark, D. B., Mercado, L. M., Sitch, S., Jones, C. D., Gedney, N., Best, M. J., Pryor, M., Rooney, G. G., Essery, R. L. H., Blyth, E., Boucher, O., Harding, R. J., Huntingford, C., and Cox, P. M.: The Joint UK Land Environment Simulator (JULES), model description – Part 2: Carbon fluxes and vegetation dynamics, *Geosci. Model Dev.*, 4, 701–722, doi:10.5194/gmd-4-701-2011, 2011. 241
- 30



## Sensitivity of snow regime in shrub-covered valley

C. B. Ménard et al.

Title Page

Abstract

Introduction

Conclusions

References

Tables

Figures

◀

▶

◀

▶

Back

Close

Full Screen / Esc

Printer-friendly Version

Interactive Discussion

- Granger, R. J., Essery, R., and Pomeroy, J. W.: Boundary-layer growth over snow and soil patches: field observations, *Hydrol. Process.*, 20, 943–951, 2006. 227, 236
- Harding, R. and Pomeroy, J.: The energy balance of the winter boreal landscape, *J. Climate*, 9, 2778–2787, 1996. 241
- 5 Hardy, J., Davis, R., Jordan, R., Ni, W., and Woodcock, C.: Snow ablation modelling in a mature aspen stand of the boreal forest, *Hydrol. Process.*, 12, 1763–1778, 1998. 226
- Hopkinson, C. and Chasmer, L.: Testing LiDAR models of fractional cover across multiple forest ecozones, *Remote Sens. Environ.*, 113, 275–288, 2009. 228
- Jia, G., Epstein, H., and Walker, D.: Spatial heterogeneity of tundra vegetation response to recent temperature changes, *Glob. Change Biol.*, 12, 42–55, 2006. 225
- 10 Kaplan, J. and New, M.: Arctic climate change with a 2°C global warming: timing, climate patterns and vegetation change, *Clim. Change*, 79, 213–241, 2006. 227
- Kirkby, M. and Weyman, D.: Measurements of contributing area in a very small drainage basin, in: Seminar Series B, No. 3, Department of Geography, University of Bristol, Bristol, 1974. 235
- 15 Kitti, H., Forbes, B. C., and Oksanen, J.: Long- and short-term effects of reindeer grazing on tundra wetland vegetation, *Polar Biol.*, 32, 253–261, 2009. 225
- Lawrence, D. M. and Swenson, S. C.: Permafrost response to increasing Arctic shrub abundance depends on the relative influence of shrubs on local soil cooling versus large-scale climate warming, *Environ. Res. Lett.*, 6, 045504, doi:10.1088/1748-9326/6/4/045504, 2011. 227, 240
- 20 Liston, G.: Local advection of momentum, heat and moisture during the melt of patchy snow covers, *J. Appl. Meteorol.*, 34, 1705–1715, 1995. 227
- Liston, G.: Representing subgrid snow cover heterogeneities in regional and global models, *J. Climate*, 17, 1381–1397, 2004. 241, 242
- 25 Liston, G. and Elder, K.: A meteorological distribution system for high-resolution terrestrial modelling, *J. Hydrometeorol.*, 7, 217–234, 2006. 235
- Liston, G. and Hiemstra, C.: Representing grass- and shrub-snow-atmosphere interactions in climate system models, *J. Climate*, 24, 2061–2079, doi:10.1175/2010JCLI4028.1, 2011. 231, 240
- 30 Liston, G., McFadden, J., Sturm, M., and Pielke, R.: Modelled changes in arctic tundra snow, energy and moisture fluxes due to increased shrubs, *Glob. Change Biol.*, 8, 17–32, 2002. 225

## Sensitivity of snow regime in shrub-covered valley

C. B. Ménard et al.

Title Page

Abstract

Introduction

Conclusions

References

Tables

Figures

◀

▶

◀

▶

Back

Close

Full Screen / Esc

Printer-friendly Version

Interactive Discussion



- Loranty, M., Goetz, S., and Beck, P.: Tundra vegetation effects on Pan-Arctic albedo, *Environ. Res. Lett.*, 6, 024014, doi:10.1088/1748-9326/6/2/024014, 2011. 225, 226
- Marsh, P. and Pomeroy, J. W.: Meltwater fluxes at an arctic forest-tundra site, *Hydrol. Process.*, 10, 1383–1400, 1996. 227
- 5 Marsh, P., Bartlett, P., Mackay, M., Pohl, S., and Lantz, T.: Snowmelt energetics at a shrub tundra site in the Western Canadian Arctic, *Hydrol. Process.*, 24, 3603–3620, doi:10.1002/hyp.7786, 2010. 226
- Mason, P. and Sykes, R.: Flow over an isolated hill of moderate slope, *Q. J. Roy. Meteor. Soc.*, 105, 383–395, 1978. 235
- 10 Ménard, C., Essery, R., Pomeroy, J., Marsh, P., and Clark, D.: A shrub bending model to calculate the albedo of shrub-tundra, *Hydrol. Process.*, 28, 341–351, doi:10.1002/hyp.9582, 2012. 226, 228, 229, 231
- Myers-Smith, I. H., Forbes, B. C., Wilmking, M., Hallinger, M., Lantz, T., Blok, D., Tape, K. D., Macias-Fauria, M., Sass-Klaassen, U., Levesque, E., Boudreau, S., Ropars, P., Her-
- 15 manutz, L., Trant, A., Collier, L. S., Weijers, S., Rozema, J., Rayback, S. A., Schmidt, N. M., Schaeppman-Strub, G., Wipf, S., Rixen, C., Menard, C. B., Venn, S., Goetz, S., Andreu-Hayles, L., Elmendorf, S., Ravolainen, V., Welker, J., Grogan, P., Epstein, H. E., and Hik, D. S.: Shrub expansion in tundra ecosystems: dynamics, impacts and research priorities, *Environ. Res. Lett.*, 6, 045509, doi:10.1088/1748-9326/6/4/045509, 2011. 237
- 20 Neumann, P. and Marsh, P.: Local advection in the snowmelt landscape of Arctic tundra, *Hydrol. Process.*, 12, 1547–1560, 1998. 227
- Oke, T.: *Boundary Layer Climates*, Routledge, London, 1987. 235
- Pajunen, A.: Environmental and biotic determinants of growth and height of arctic willow shrubs along a latitudinal gradient, *Arct. Antarct. Alp. Res.*, 41, 478–485, 2009. 225
- 25 Pomeroy, J. and Li, L.: Prairie and Arctic areal snow cover mass balance using a blowing snow model, *J. Geophys. Res.*, 105, 26619–26634, 2000. 234
- Pomeroy, J., Gray, D., Shook, K., Toth, B., Essery, R., Pietroniro, A., and Hedstrom, N.: An evaluation of snow accumulation and ablation processes for land surface modelling, *Hydrol. Process.*, 12, 2339–2367, 1998. 238, 241
- 30 Pomeroy, J., Toth, B., Granger, R., Hedstrom, N., and Essery, R.: Variation in surface energetics during snowmelt in a subarctic mountain catchment, *J. Hydrometeorol.*, 4, 702–719, 2003. 227, 234

## Sensitivity of snow regime in shrub-covered valley

C. B. Ménard et al.

Title Page

Abstract

Introduction

Conclusions

References

Tables

Figures

◀

▶

◀

▶

Back

Close

Full Screen / Esc

Printer-friendly Version

Interactive Discussion



Pomeroy, J., Essery, R., and Toth, B.: Implications of spatial distributions of snow mass and melt rate on snow-cover depletion: observations in a subarctic mountain catchment, *Ann. Glaciol.*, 38, 195–201, 2004. 225, 238, 241

Pomeroy, J., Bewley, D., Essery, R., Hedstrom, N., Link, T., Granger, R., Sicart, J.-E., Ellis, C., and Janowicz, R.: Shrub tundra snowmelt, *Hydrol. Process.*, 20, 923–941, 2006. 226, 228, 241

Press, W., Teukolsky, S., Vetterling, W., and Flannery, B.: *The Art of Scientific Computing, Numerical recipes in Fortran 77*, 2nd edn., Cambridge University Press, Cambridge, 1996. 245

Quinton, W. L., Carey, S. K., and Goeller, N. T.: Snowmelt runoff from northern alpine tundra hillslopes: major processes and methods of simulation, *Hydrol. Earth Syst. Sci.*, 8, 877–890, doi:10.5194/hess-8-877-2004, 2004. 238

Raynolds, M., Walker, D., and Maier, H.: NDVI patterns and phytomass distribution in the circumpolar Arctic, *Remote Sens. Environ.*, 102, 271–281, 2006. 225

Roesch, A., Wild, M., Gilgen, H., and Ohmura, A.: A new snow fraction parametrization for the ECHAM4 GCM, *Clim. Dynam.*, 17, 933–946, 2001. 241

Sellers, P., Mintz, Y., Sud, Y., and Dalcher, A.: A Simple Biosphere model (SiB) for use in general circulation models, *J. Atmos. Sci.*, 43, 505–531, 1986. 227

Sturm, M., McFadden, J., Liston, G., Chapin III, F., Racine, C., and Holmgren, J.: Snow-shrub interactions in arctic tundra: a hypothesis with climatic implications, *J. Climate*, 14, 336–344, 2001. 225

Sturm, M., Douglas, T., Racine, C., and Liston, G.: Changing snow and shrub conditions affect albedo with global implications, *J. Geophys. Res.*, 110, G01004, doi:10.1029/2005JG000013, 2005a. 225, 226, 241

Sturm, M., Schimel, J., Michaelson, G., Welker, J. M., Oberbauer, S. F., Liston, G. E., Fahnestock, J., and Romanovsky, V. E.: Winter biological processes could help convert arctic tundra to shrubland, *Bioscience*, 55, 17–26, 2005b. 226, 241

Tape, K., Sturm, M., and Racine, C.: The evidence for shrub expansion in northern Alaska and the Pan-Arctic, *Global Change Ecology*, 12, 686–702, 2006. 225, 237

Tape, K., Lord, R., Marshall, H., and Ruess, R. W.: Snow-mediated ptarmigan browsing and shrub expansion in arctic Alaska, *Ecoscience*, 17, 186–193, 2010. 225

Tremblay, B., Levesque, E., and Boudreau, S.: Recent expansion of erect shrubs in the Low Arctic: evidence from eastern Nunavik, Environ. Res. Lett., 7, 035501, doi:10.1088/1748-9326/7/3/035501, 2012. 225

5 Versegny, D.: CLASS – a Canadian land surface scheme for GCMS, I: Soil model, Int. J. Climatol., 11, 111–133, 1991. 227

Warren, S.: Optical properties of snow, Rev. Geophys. Space GE, 20, 67–89, 1982. 226

Yang, Z.-L., Dickinson, R. E., Robock, A., and Vinnikov, K.: On validation of the snow sub-model of the biosphere-atmosphere transfer scheme with Russian snow cover and meteorological observational data, J. Climate, 10, 353–373, 1997. 231

## HESSD

11, 223–263, 2014

### Sensitivity of snow regime in shrub-covered valley

C. B. Ménard et al.

Title Page

Abstract

Introduction

Conclusions

References

Tables

Figures

◀

▶

◀

▶

Back

Close

Full Screen / Esc

Printer-friendly Version

Interactive Discussion



## Sensitivity of snow regime in shrub-covered valley

C. B. Ménard et al.

**Table 1.** 3SOM mean and root mean square errors, bias and correlation coefficient of sensible, latent and ground heat fluxes at the tall and short shrubs sites in 2003 and 2004.

	LE				H				G			
	Mean	RMS	Bias	$r^2$	Mean	RMS	Bias	$r^2$	Mean	RMS	Bias	$r^2$
Short shrubs site 2003	7.2	18.0	0.47	0.73	-21.9	53.7	-0.42	0.78	18.3	47.5	2.0	0.41
Tall Shrubs site 2003	17.9	26.2	1.50	0.72	-3.2	64.1	-0.06	0.76	-	-	-	-
Short shrubs site 2004	-1.6	14.9	-0.08	0.66	-12.7	50.3	-0.90	0.64	-	-	-	-
Tall shrubs site 2004	11.0	21.7	0.91	0.42	-7.7	62.3	-0.21	0.72	-	-	-	-

Title Page

Abstract

Introduction

Conclusions

References

Tables

Figures

⏪

⏩

◀

▶

Back

Close

Full Screen / Esc

Printer-friendly Version

Interactive Discussion



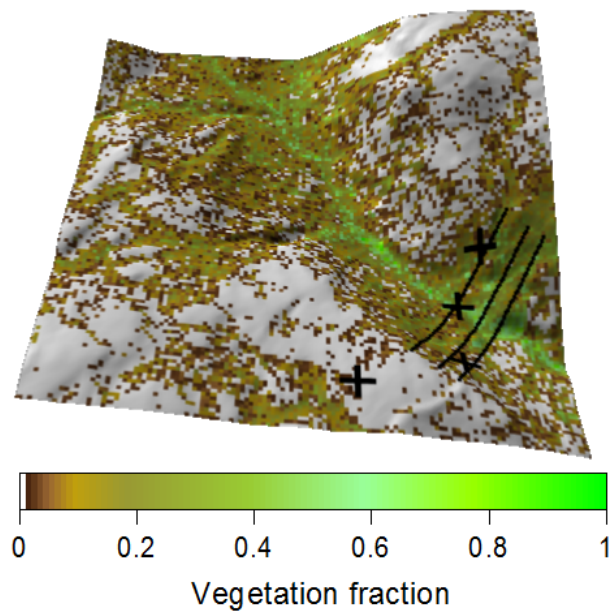
## Sensitivity of snow regime in shrub-covered valley

C. B. Ménard et al.

**Table 2.** Coupled model bias, mean error, root mean square (RMS) and RMS errors normalized by the standard deviation of measured snow depths, for snow depths on the three dominant topographical units and at different stages of the melt season (Pre-melt = 21 April; Melt = 25 April, 28 April, 3 May and 7 May; End of Melt = 10 May, 16 May and 19 May. Only one of the three transects was surveyed on the last two dates).

	Bias			RMSE			NRMSE			ME		
	NFS	Valley	SFS	NFS	Valley	SFS	NFS	Valley	SFS	NFS	Valley	SFS
Pre-melt	-0.01	0.07	0.10	0.40	0.17	0.30	1.03	1.09	0.74	-0.01	0.05	0.07
Melt	-0.07	0.25	0.73	0.46	0.25	0.42	1.11	1.01	0.86	-0.06	0.11	0.2
End of melt	0.41	-0.39	-0.16	0.53	0.27	0.34	1.13	0.98	0.75	-0.31	-0.11	-0.02

[Title Page](#)
[Abstract](#)
[Introduction](#)
[Conclusions](#)
[References](#)
[Tables](#)
[Figures](#)
[Back](#)
[Close](#)
[Full Screen / Esc](#)
[Printer-friendly Version](#)
[Interactive Discussion](#)

**Fig. 1.** 8 m resolution LiDAR based digital elevation map of the 1 km × 1 km area around the valley in the Granger basin, overlaid by a vegetation fraction map. Four meteorological stations (from north to south: south-facing, tall shrubs, north-facing and short shrubs stations) and the three snow depth transects are shown in black.

## Sensitivity of snow regime in shrub-covered valley

C. B. Ménard et al.

Title Page

Abstract

Introduction

Conclusions

References

Tables

Figures

⏪

⏩

◀

▶

Back

Close

Full Screen / Esc

Printer-friendly Version

Interactive Discussion



## Sensitivity of snow regime in shrub-covered valley

C. B. Ménard et al.

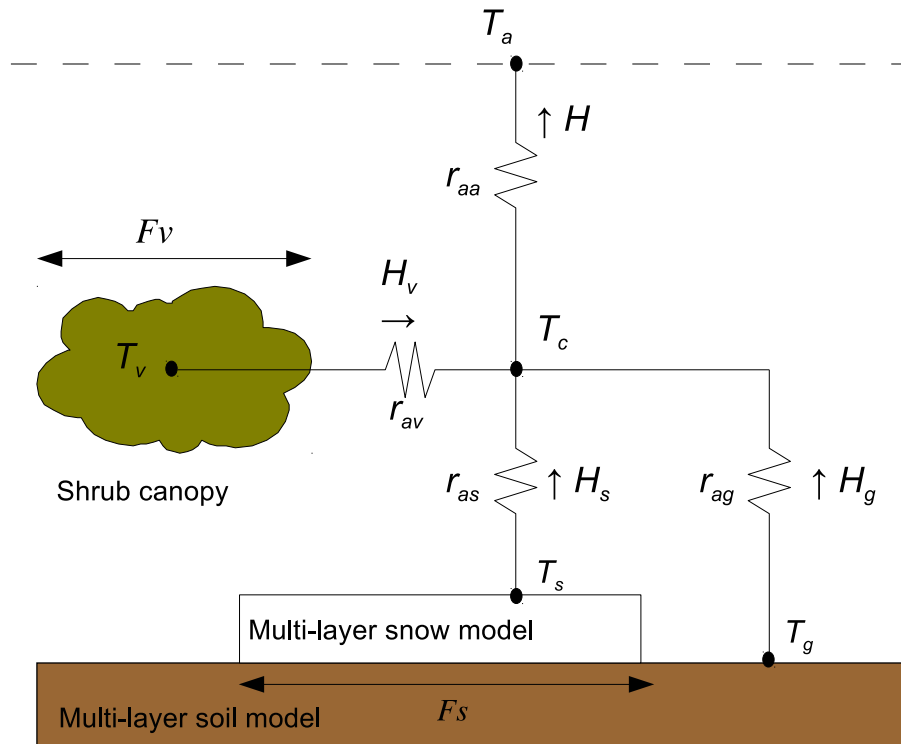


**Fig. 2.** Structure of 3SOM with reference to the heat exchanges and the resistance network.

Title Page

Abstract	Introduction
Conclusions	References
Tables	Figures

⏪ ⏩  
⏴ ⏵  
Back Close

Full Screen / Esc

Printer-friendly Version  
Interactive Discussion



## Sensitivity of snow regime in shrub-covered valley

C. B. Ménard et al.

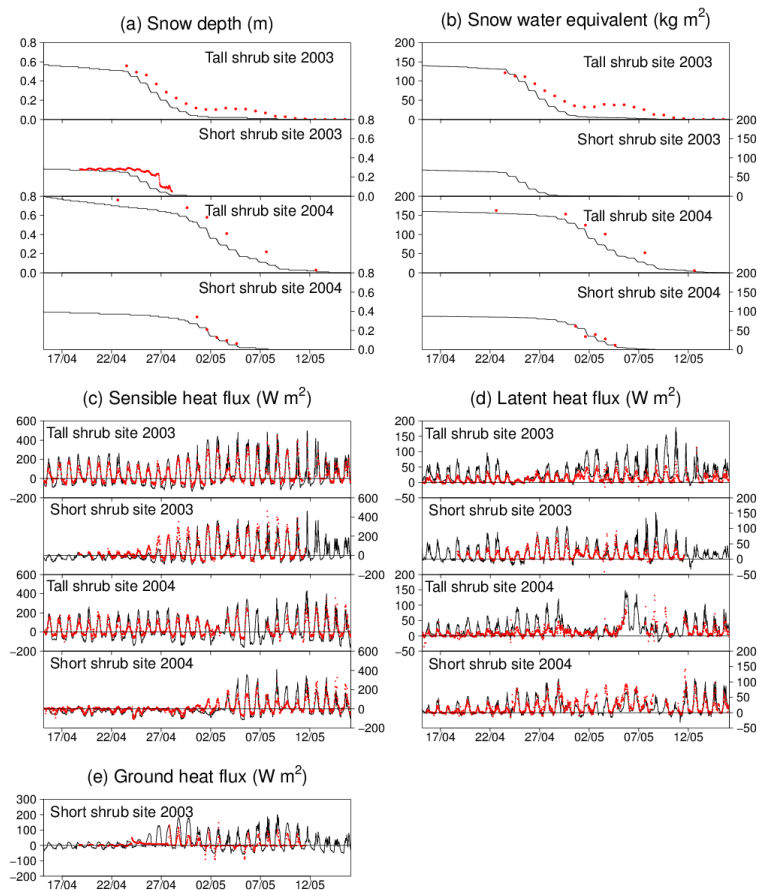


**Fig. 3.** Measured (dots) and modelled (lines) **(a)** snow depth, **(b)** snow water equivalent, **(c)** sensible heat flux, **(d)** latent heat flux and **(e)** ground heat flux during snowmelt in 2003 and 2004. Snow depth and water equivalent measurements were manual (automatic snow depth at the short shrubs site in 2003) and fluxes were measured using eddy correlation systems.

## Sensitivity of snow regime in shrub-covered valley

C. B. Ménard et al.

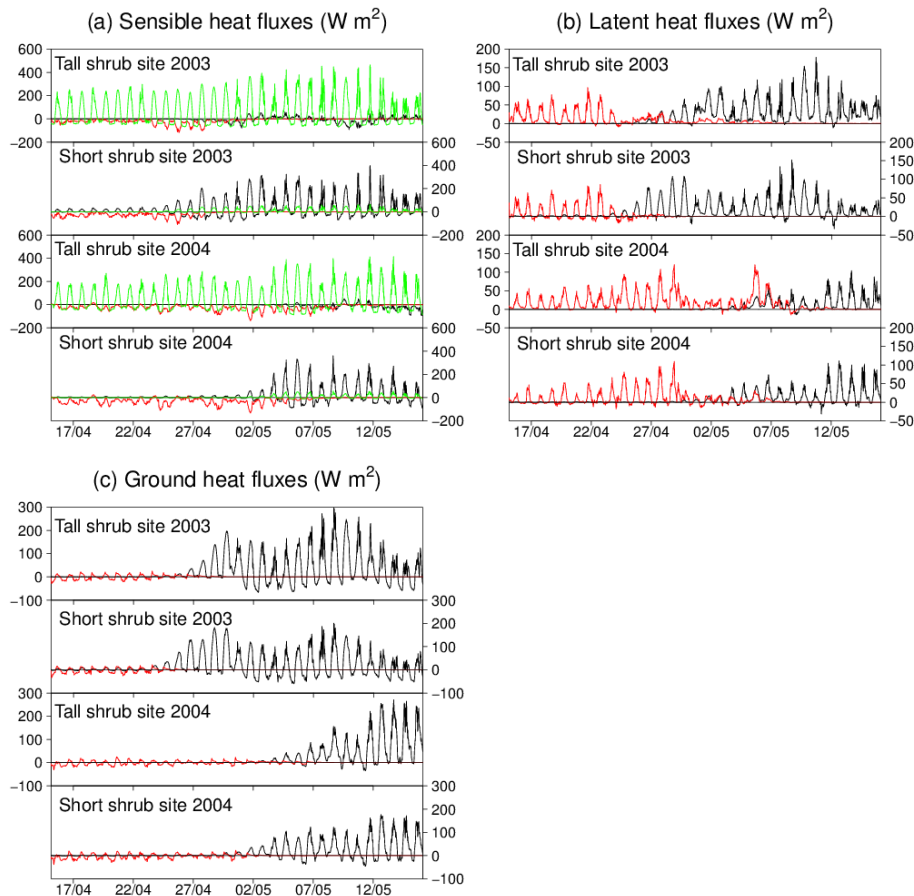


**Fig. 4.** Modelled (a) sensible heat fluxes, (b) latent heat fluxes and (c) ground heat fluxes over individual sources (black = ground, red = snow, green = shrub) at the tall and short shrub sites in 2003 and 2004.

## Sensitivity of snow regime in shrub-covered valley

C. B. Ménard et al.

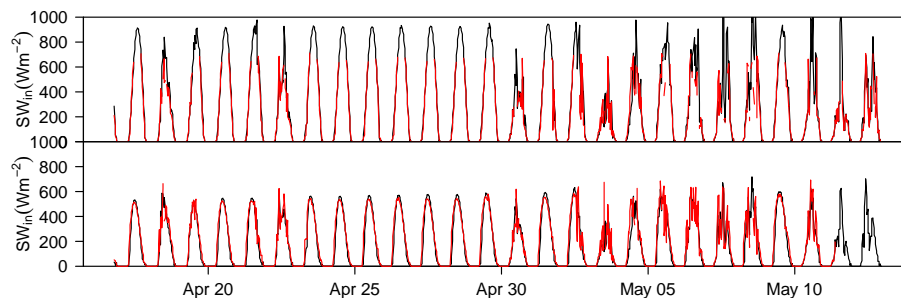


**Fig. 5.** Modelled (black) and measured (red) incoming shortwave radiation at the two slope stations in spring 2003 (**a**, southwest-facing slope; **b**, northeast-facing slope).

[Title Page](#)[Abstract](#)[Introduction](#)[Conclusions](#)[References](#)[Tables](#)[Figures](#)[◀](#)[▶](#)[◀](#)[▶](#)[Back](#)[Close](#)[Full Screen / Esc](#)[Printer-friendly Version](#)[Interactive Discussion](#)

## Sensitivity of snow regime in shrub-covered valley

C. B. Ménard et al.

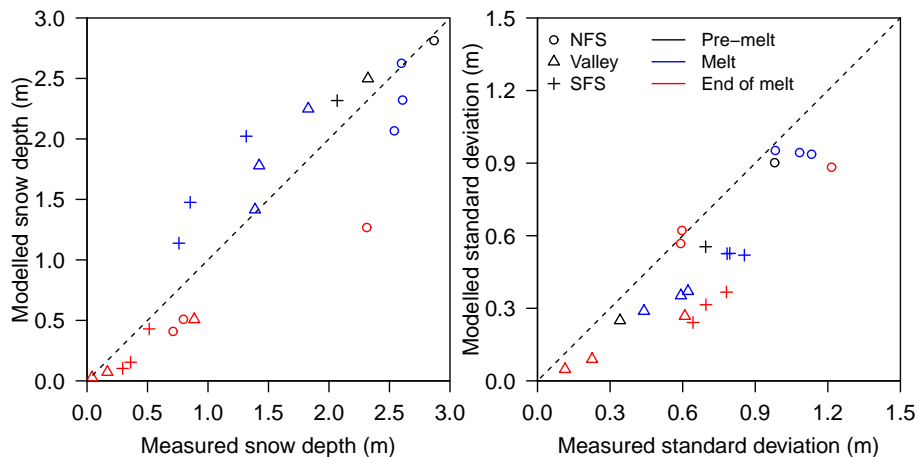


**Fig. 6.** Modelled vs. measured average snow depths and standard deviation of snow depth on the northeast facing slope (NFS), the valley bottom and the southwest-facing slope (SFS) before, during and at the end of the melt season.

Title Page

Abstract

Introduction

Conclusions

References

Tables

Figures

◀

▶

◀

▶

Back

Close

Full Screen / Esc

Printer-friendly Version

Interactive Discussion



---

**Sensitivity of snow regime in shrub-covered valley**C. B. Ménard et al.

---

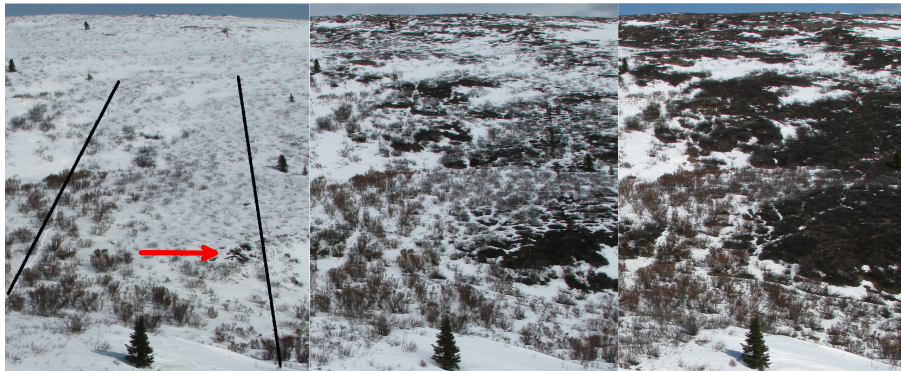


**Fig. 7.** Area surrounding the two easternmost transects on the southwest-facing slope on 20 April, 27 April and 3 May 2008 from left to right. The visible portion of the transects is approximately 200 m long. The red arrow is pointing to a snow-free patch.

[Title Page](#)[Abstract](#)[Introduction](#)[Conclusions](#)[References](#)[Tables](#)[Figures](#)[|◀](#)[▶|](#)[◀](#)[▶](#)[Back](#)[Close](#)[Full Screen / Esc](#)[Printer-friendly Version](#)[Interactive Discussion](#)

## Sensitivity of snow regime in shrub-covered valley

C. B. Ménard et al.

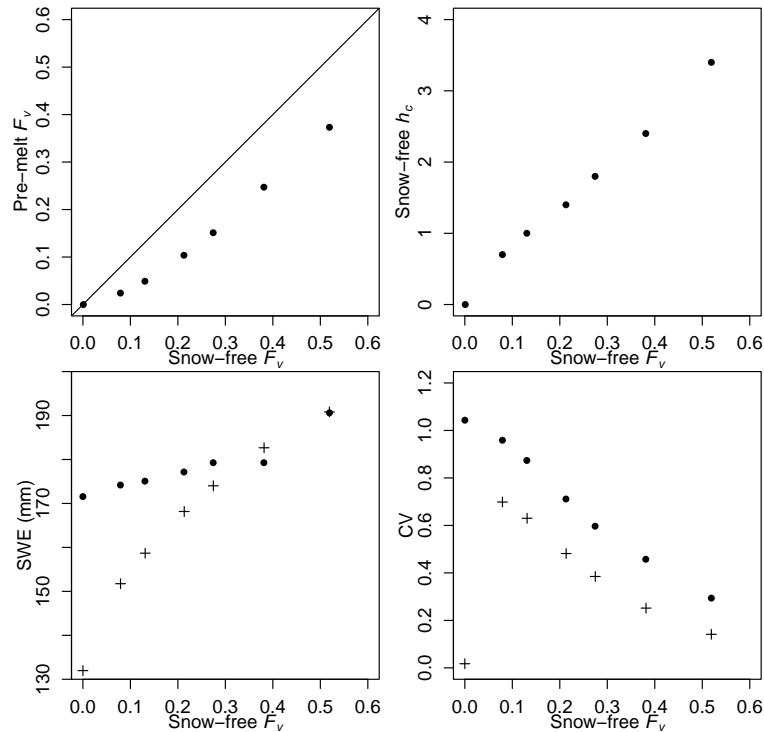


**Fig. 8.** Exposed vegetation fraction, vegetation height, mean SWE and coefficient of variation in SWE on 22 April as functions of snow-free vegetation fraction for runs with (dots) and without (crosses) topography.

[Title Page](#)
[Abstract](#)
[Introduction](#)
[Conclusions](#)
[References](#)
[Tables](#)
[Figures](#)
[◀](#)
[▶](#)
[◀](#)
[▶](#)
[Back](#)
[Close](#)
[Full Screen / Esc](#)
[Printer-friendly Version](#)
[Interactive Discussion](#)


## Sensitivity of snow regime in shrub-covered valley

C. B. Ménard et al.

Title Page

Abstract

Introduction

Conclusions

References

Tables

Figures

◀

▶

◀

▶

Back

Close

Full Screen / Esc

Printer-friendly Version

Interactive Discussion

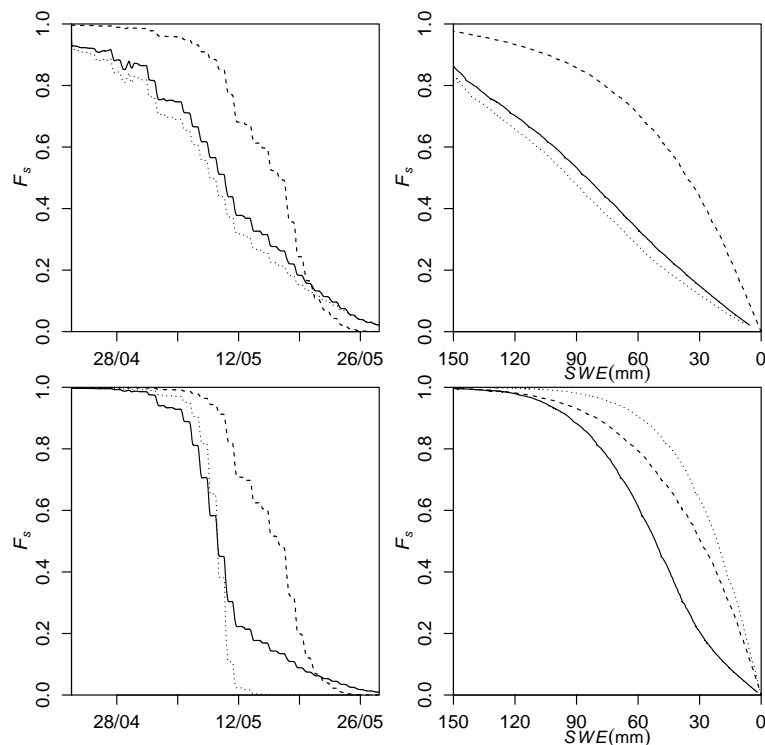


**Fig. 9.** Time series of snow cover fraction (left) and snow cover depletion curves (right) from runs with (top) or without (bottom) topography and vegetation fractions of 0 (dotted lines), 0.08 (solid lines) or 0.52 (dashed lines).

## Sensitivity of snow regime in shrub-covered valley

C. B. Ménard et al.

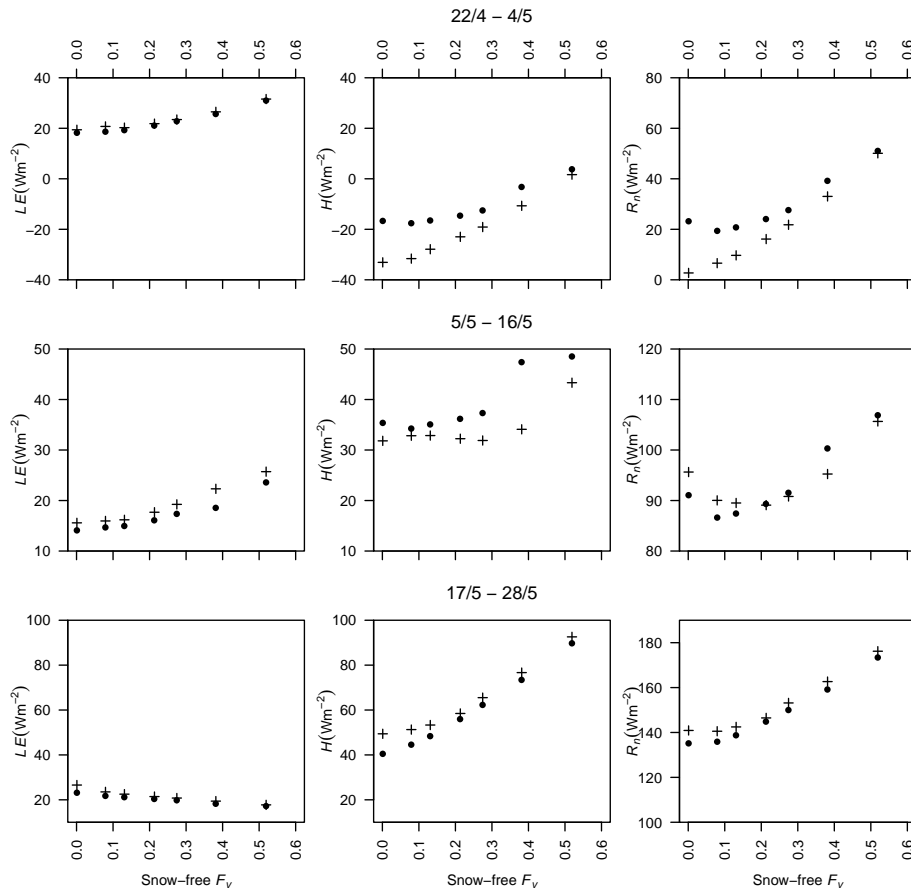


**Fig. 10.** Area averaged latent heat flux, sensible heat flux and net radiation as functions of snow-free vegetation fraction for runs with (dots) and without (crosses) topography over three time periods.

Title Page

Abstract

Introduction

Conclusions

References

Tables

Figures

◀

▶

◀

▶

Back

Close

Full Screen / Esc

Printer-friendly Version

Interactive Discussion

